MONOFRACTALITY IN RR HEART RATE BY MULTIFRACTAL TOOLS*

Danuta Makowiec†, Aleksandra Dudkowska

Institute of Theoretical Physics and Astrophysics, University of Gdańsk
Wita Stwosza 57, 80–952 Gdańsk, Poland

Rafał Gałąska, Andrzej Rynkiewicz, Joanna Wdowczyk-Szulc

1st Department of Cardiology, Medical University of Gdańsk
Dębinki 7, 80–952 Gdańsk, Poland

(Received May 5, 2009)

Multifractal formalism is tested if it can work as a robust estimator of monofractals when scaling intervals are fixed. Intervals for scaling are selected to be consistent with known frequency bands of power spectral analysis used in estimates of heart rate variability: low frequency (LF), very low frequency (VLF), and ultra low frequency (ULF). Tests on fractional Brownian motions and a binomial cascade are performed to validate popular multifractal methods: Wavelet Transform Modulus Maxima and Multifractal Detrended Fluctuation Analysis. Then the methods are applied to identify monofractal elements of control processes driving the heart rate. A transition is found in the dynamic organization of autonomic nervous system control of the heart rate related to the change in scaling intervals. The control over the diurnal heart rate is of a multifractal type when considered in LF and of a monofractal type when observed in ULF. Additionally, this transition affects on a switch in a relation between widths of diurnal and nocturnal multifractal spectra.

PACS numbers: 95.75.Wx, 87.90.+y, 89.75.Da, 05.65.+b

1. Introduction

Frequency of heart contractions is mediated by two parts: sympathetic and parasympathetic, of autonomic nervous system (ANS) and hormonal (rennin–angiotensin–aldosterone system) activity [1–5]. Since discovering

* Presented at the XXI Marian Smoluchowski Symposium on Statistical Physics Zakopane, Poland, September 13–18, 2008.

† fizdm@univ.gda.pl

the relation between heart rate variability (HRV) and the state of ANS, wide investigations have been continued to specify this connection. Conventionally it is done by developing time- and frequency-characteristics derived from analysis of signals consisting of time intervals between subsequent heart contractions (RR-intervals) [1]. Because of our increasing understanding of complex systems, so-called, non-linear indices have been proposed [6–8] and then included into the set of standard markers of HRV [9]. Multifractal analysis has been found as a promising source of new assessments of HRV [10–17].

Power spectral analysis of normal heart rate has gained popularity because it is believed that by this analysis we are able to measure dynamic changes in the ANS control of heart rate [1]. The reduced levels of the spectral power have been identified as predictors of all-cause mortality (see [5] for discussion). Traditionally the power spectral analysis is performed in two bands: high-frequency (HF: 0.15–0.4 Hz) and low-frequency (LF: 0.04–0.15 Hz). The HF band is attributed to parasympathetic modulation. The LF band appears to be jointly mediated by both parts of ANS: parasympathetic and sympathetic. The physiological meaning of the two other ranges of power spectrum: very-low-frequency (VLF: 0.004–0.04 Hz) and ultra-low-frequency (ULF: $\leq$ 0.004 Hz) is less clear. There are evidences that these bands are influenced by thermoregulatory mechanisms and humoral rennin–angiotensin system. However a physical activity affects them too [18].

The power spectrum in the VLF and ULF bands has a power-law form, *i.e.*, it decays like $1/f^{\beta}$ where f is frequency [6–8]. If a healthy heart rhythm is analyzed then β is close to 1. But in the case of the heart failure β becomes significantly greater than 1. Therefore, β is considered as a marker of autonomic control [20]. Similar markers which would be related to the HF and/or LF bands are awaited. Efforts are made to quantify properties of short-time scales by, for example, discussing fluctuations of RR-signals in scales of few contractions [19–21]. Calls can be found for further research to discover the nonlinear indices with clear physiological meaning [5, 21, 22].

In the case of stationary processes, a power-law decay of the spectral density is directly related to the slow decay of autocorrelation function. It is said that the stationary process is driven by long range dependences (LRD). Moreover, any process having LRD, asymptotically, becomes a monofractal, *i.e.*, in large time scales the process is self-similar with the self-similarity index H determined by β: $H = (\beta + 1)/2$ [23, 24]. This way monofractal properties found in a signal provide a direct understanding to dynamics of a studied system. The potential of monofractal analysis is far from being fully exploited [25].

LRD leave the features of short-time scales essentially unspecified. The multifractal analysis allows to get insights on these local irregularities [23]. Unfortunately, the multifractal analysis cannot be applied as a black box.

It involves sophisticated mathematical tools and as a result numerical procedures are sensitive to many known (such as finite size of signals) and unknown (*e.g.*, so-called linearization effect [26]) reasons. The relation between properties expected from rigorous investigations and properties received from a numerical approach is the accepted measure of the quality of multifractal tools [15, 16, 26–29].

Following this idea, in the present paper we examine how two popular multifractal methods: Wavelet Transform Modulus Maxima (WTMM) [27] and Multifractal Detrended Fluctuation Analysis (MDFA) [28] map monofractality. In particular, we test in what way multifractal properties of the most popular monofractal processes, *i.e.*, fractional Brownian motions (fBm), are represented when the multifractal analysis is performed in time scales corresponding to physiologically grounded frequency bands: LF, VLF and ULF. Unfortunately, due to high numerical errors the HF band appears as not accessible.

In our estimates we will use some of indices of monofractality studied by us earlier [15, 17, 30]. However, in the present paper, the robust method to distinct a monofractal from a multifractal will be proposed. Then we apply results of our tests to heart rate signals to discover monofractal elements in series of RR-intervals of normal sinus rhythm of a healthy man. Our basic concern is whether complexity of HRV, if investigated in particular time intervals: LF: 10–30 heart beats, VLF: 30–300 heart beats and ULV: over 300 heart beats, can be approximated by some fractional Brownian motion. Changes in HRV will be discussed considering influence of the circadian rhythm. Namely, we consider separately data corresponding to the diurnal activity and data describing the nocturnal rest.

The paper is organized as follows. In Section 2, after a short introduction to the mathematics of the multifractal formalism, we present the method how to distinguish a monofractal signal from a multifractal one. We start with fixing necessary properties for a multifractal spectrum to be read as a representative for some fBm, Subsection 2.2. We show by simulation tests that this method improves the quality of numerical results, Subsection 2.3. Then we report tests performed how WTMM and MDFA methods represent monofractality if scaling intervals are limited, Subsection 2.4. Finally, in Section 3 we show and discuss the results of the methods in discovering monofractal ingredients in RR signals. In the following we operate with the same series of RR-intervals that were considered in our previous studies [15, 17]. These old results are partially restored in the present paper when we investigate multifractal properties in the ULF band. Preliminary investigations about effects on multifractality caused by change of a scaling interval can be found in [30]. In the last section we collect and conclude our observations.

2. Set of spectrum accumulation points

2.1. Quantities for scaling

As it was mentioned the multifractal formalism is a nice piece of sophisticated mathematics. Therefore, it is instructive to start with a short review of rigorous mathematics to understand better limits of numerical approximations and to be ensured that any change in these approximations demands validations. The review is based on [23, 27, 28].

The mathematical meaning of multifractality arises from the notion of pointwise regularity of a continuous function $X(t)$. Namely, for any t_0 one searches for a maximal value $h(t_0)$ such that

$$|X(t_0+\delta t) - X(t_0)| < C|\delta t|^{h(t_0)} \tag{2.1}$$

for some $C > 0$ and if $\delta t \to 0$. Notice that if a signal $X(t)$ is differentiable at t_0 then $h(t_0) = 1$. If $h(t_0) \geq 1$ then the neighboring values of $X(t)$ are similar to $X(t_0)$, while if $h(t) < 1$ then in any neighborhood of $X(t_0)$ the wide set of values of $X(t)$ can appear.

Then one asks what is the structure of a subset $E(h) = \{t_0 : h(t_0) = h\}$ that collects points of the domain where the exponent $h(t_0)$ in (2.1) is equal to a given value h. By changing h one obtains a family of sets $E(h)$ which decomposes the domain of $X(t)$ according to the singularity exponents of a signal. In the case of multifractal signals each set $E(h)$ has a complex — fractal structure, and sets $E(h)$ are highly interwoven. The structure of each set $E(h)$ is assessed by its Hausdorff dimension:

$$D(h) = \dim_{\mathrm{H}}\{E(h)\}\,. \tag{2.2}$$

By a multifractal spectrum one calls a function $h \to D(h)$. Hence if a signal X is differentiable everywhere then the multifractal spectrum is reduced to a single point $(1, 1)$.

Direct numerical calculations, going by (2.1) and (2.2) to a multifractal spectrum, are extremely difficult. Fortunately, they can be simplified thanks to the multifractal formalism. The multifractal formalism is based on the relation between multifractal spectrum of $X(t)$ and so-called *scaling exponent function* $\tau(q)$ received from estimates of scaling properties of partition functions calculated for $X(t)$.

Let $\{X(i)\}_{i=1,2,\ldots}$ be a discrete approximation to a sample path of some stochastic process $X(t)$. Let the series $\{X(i)\}$ be divided into boxes consisting of n points. Any quantity $R_X^{(n)}(k)$ which describes some property of a signal in a k-th box is called the multiresolution quantity. It is said that X possesses scaling properties if the partition function, *i.e.*, the averages of q moments of a given multiresolution quantity, depend on a scale n in the power-law form, namely:

$$\frac{1}{K}\sum_{k=1}^{K}\left|R_X^{(n)}(k)\right|^q \propto |n|^{\tau(q)}\,, \tag{2.3}$$

where $\tau(q)$ is the scaling exponent function. The multifractal spectrum $(h, D(h))$ is obtained by the Legendre transform applied to the scaling exponent function $(q, \tau(q))$:

$$h = \frac{d\tau(q)}{dq}\,, \qquad D(h) = qh - \tau(q)\,. \tag{2.4}$$

Again, the direct usage of (2.3) and (2.4) suffers from numerical difficulties what often effects in wrong estimates. However, after wide simulations (see *e.g.* [28, 29]) the following two numerical methods, though only related intuitively to rigorous mathematics, are used to calculate multifractal spectra.

The first method is called the Wavelet Transform Modulus Maxima (WTMM) method [27]. The wavelet coefficient of the wavelet transform of a signal X is chosen as a multiresolution quantity: $R_{X,\psi}^{(n)}(k)$, ψ denotes the mother wavelet transformed to a scale n and shifted to a k-th box. But the partition function is constructed differently from (2.3). In a given scale n a set of the local maxima of a function $k \longrightarrow |R_{X,\psi}^{(n)}(k)|$ is determined. Then at a given time position the maxima are chained across scales to establish, so-called, maxima lines. The partition function $Z(n, q)$ is formed from the largest multiresolution quantities along the maxima lines, *i.e.*:

$$Z(n,q) = \sum_{k:\sup \substack{\text{local maxima}\\ \text{across scales}}} \left|R_{X,\psi}^{(n)}(k)\right|^q\,. \tag{2.5}$$

A multiresolution quantity of the second method called Multifractal Detrended Fluctuation Analysis (MDFA) [28], estimates departures of the signal X from a local polynomial trend: $R_{X,P_m^k}^{(n)}(k)$ where P_m^k is a polynomial trend of m order found for the k-th box:

$$R_{X,P_m^k}^{(n)}(k) = \left(\sum_{i=kn+1}^{(k+1)n}\left[X(i) - P_m^k(i)\right]^2\right)^{\frac{1}{2}}\,. \tag{2.6}$$

The partition function $F(n, q)$ is given as

$$F(n,q) = \sum_{k=1}^{K}\left(R_{X,P_m^k}^{(n)}(k)\right)^q\,. \tag{2.7}$$

Notice that the partition function (2.7) differs from (2.3) and the original one given in [28] by absence of the coefficient $1/K$. Thanks to this modification the scaling exponent functions $\tau(q)$ provided by (2.5) or (2.7) are exactly the same.

In the following we will call a multifractal spectrum calculated on the base of $Z(n,q)$ as a WTMM spectrum and a multifractal spectrum received from $F(n,q)$ as a MDFA spectrum.

2.2. Monofractality by multifractal estimators

A self-similar process with a self-similarity index H gives a point multifractal spectrum located at $(H,1)$. Fractional Brownian motions fBm_H are the simplest self-similar processes with the self-similarity index $H \in (0,1)$. Hence a sample path of fBm_H has everywhere a local singularity exponent h equal to H. Moreover, a multifractal spectrum of a process of integrated values of $\mathrm{fBm}_H(i)$: $\mathrm{fBm}_H^{\mathrm{int}}(k) = \sum_{i=0,\ldots,k} \mathrm{fBm}_H(i)$ is a point too. The point of a spectrum takes the value $(H^{\mathrm{int}} = 1 + H, 1)$.

The quality of multifractal tools — methods WTMM and MDFA, will be assessed according to their representation of a point spectrum of fBm_H, namely, by:

(a) the distance between the expected value and the value at which the maximum of a multifractal spectrum is attained,

(b) the width of the multifractal spectrum.

Moreover, we also check

(c) how the properties (a) and (b) are represented if multifractal spectra are received from integrated signals $\mathrm{fBm}_H^{\mathrm{int}}(k)$

(d) the dependence between the properties (a)–(c) and the interval where the scaling (2.3) is performed.

The direct estimates of the described features experience difficulties related to shapes of numerically calculated multifractal spectra. Typically a multifractal spectrum has a parabola-like shape. Identification of the spectrum maximum is not difficult. But it also happens that a spectrum looks like a parabola modified by some mirror and/or rotation transformations. In such a case determination of the maximum is not obvious. Moreover it often occurs that one of the wings of a spectrum is enormously wide. Then calculations of the width of a spectrum needs special effort. For these reasons we propose to consider the following procedure to quantify a multifractal spectrum:

- Let us consider a set of singularity exponents $\{h_i\}$ obtained numerically according to the formula (2.4). Namely, if $q_i = q_0 + i\Delta q$ and $\Delta q > 0$ is small enough, then we have:

$$h_i = \Delta\tau(q_i)/\Delta q = [\tau(q_i + \Delta q) - \tau(q_i)]/\Delta q\,. \tag{2.8}$$

  Let a function $\mathrm{pdf}(h_i)$ describe the probability that h_i occurs in the set of $\{h_i\}$. Each local peak in pdf will be called *a spectrum accumulation point* and denoted h_{acc}.

We expect that in the case of fBm_H and $\mathrm{fBm}_H^{\mathrm{int}}$ signals we obtain only a single spectrum accumulation point h_{acc} and its value coincides with the maximum in a multifractal spectrum. Thus, $h_{\mathrm{acc}} = H$ for fBm_H series and $h_{\mathrm{acc}} = 1 + H$ for $\mathrm{fBm}_H^{\mathrm{int}}$.

2.3. Validation of the spectrum accumulation point approach

In the following subsection we discuss how the set of spectrum accumulation points represents a multifractal spectrum. We show also that this approach provides a robust procedure of recognizing monofractality.

It is not surprising that a set of accumulation spectrum points should depend on the interval of q where a partition function is calculated. To check the q-interval influence we compare pdfs received when different q-intervals are considered. We decide to present results obtained from series with $H = 0.2$ because the heart rate signals are known to be related to this value. Moreover, we deal with series consisting of 25000 points because signals with RR-intervals have the similar lengths

For the three samples of $\mathrm{fBm}_{0.2}$ (produced by tsfBm software [31]) the partition functions $F(n, q)$ and $Z(n, q)$ (using Physionet software [32]) were found for all $|q| < 50$, with a step $\Delta q = 0.1$. The scaling exponent functions $\tau(q)$ were calculated for scales $n > 100$, *i.e.*, in the scaling interval usually used in multifractal estimates. In the first row of Fig. 1 we present the scaling exponent functions $\tau(q)$ and the MDFA and WTMM spectra. Below the pdfs of these spectra are shown. The size of a bin is $\Delta h = 0.02$.

If $|q|$ is large then each negative ($q < 0$) and positive ($q > 0$) part of $\tau(q)$ separately can be fitted very accurately by a linear function. Therefore the corresponding pdf has two accumulation points located at the limits of the spectrum, see grey (yellow on-line) boxes in Fig. 1. But values of these accumulation points are weakly depended on the expected value and they variate from a sample to a sample. Variability in the limit behavior of $\tau(q)$ means that we are outside the q-interval where the multifractal formalism is valid. It is said that the scaling exponent function $\tau(q)$ suffers from the linearization effect [26].

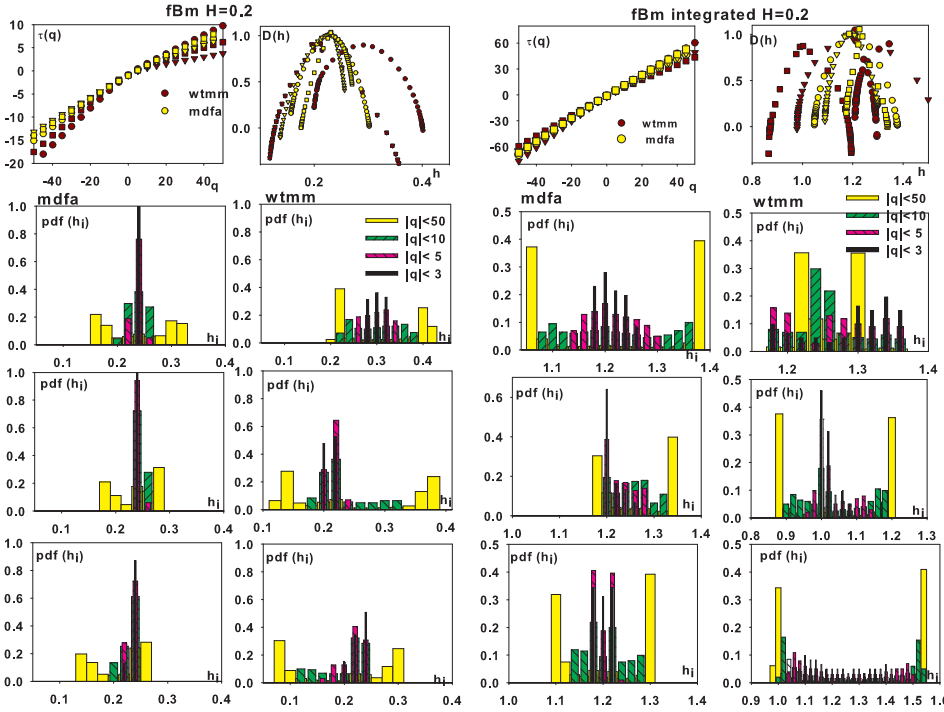

Fig. 1. Multifractal analysis results obtained by MDFA and WTMM together with corresponding pdf functions for three samples of $\mathrm{fBm}_{0.2}$. The first row contains plots of the scaling exponent functions and multifractal spectra received by both estimators for pure (left part) and integrated (right part) signals. Below pdfs are plotted when an interval of qs is subsequently limited.

When $|q|$-interval is narrower, *e.g.*, $|q| < 10$, see dark grey striped (green on-line) boxes in Fig. 1, then most of the distributions of h_is become a cap-like. Only WTMM spectra received from integrated signals still give wide distributions of a cup-like. Thus the set of spectrum accumulation points has been changed due to the change in the q-interval — two limiting accumulation points have disappeared, and a single accumulation point has emerged. When q-interval is squeezed further then the value of the maximum in pdf grows. In the case of $|q| < 3$, we see sharp peaks determining h_{acc} as located close to 0.2 for $\mathrm{fBm}_{0.2}$ signals, and to 1.2 in the case of $\mathrm{fBm}^{\mathrm{int}}_{0.2}$ series (see black boxes in Fig. 1). Unfortunately this observation is not true in the case of the WTMM method applied to integrated signals.

Thus the proposed marker of monofractality can be trapped by the linearization effect. To limit the influence of this trap, the interval of q should be chosen to be close to 0. However, one can ask if by squeezing the interval

of q we do not weaken our possibility to discover multifractality. To test how much we can limit the q interval in a safe way, let us observe the set of spectrum accumulation points received from a discrete approximation of the binomial cascade, see Fig. 2.

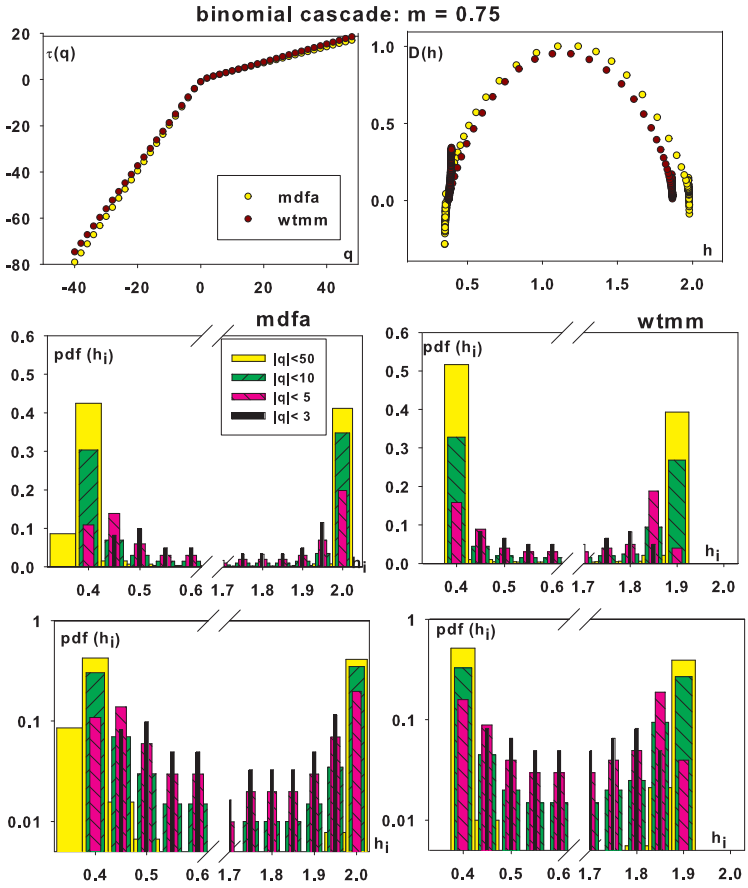

Fig. 2. Multifractal analysis results received for a binomial cascade signal with $m = 0.75$. The first row contains plots of the scaling exponent functions and multifractal spectra calculated by both estimators. Below pdfs are plotted for interval of q subsequently restricted. The bottom pdf plots are in log-scale to emphasize the pdf values inside the spectra interval. The bin size is 0.05. Theoretical limits are 0.415 and 2.0.

A binomial cascade signal is known from its transparent multifractal properties. It is constructed through the multiplicative iterations characterized by m parameter, see *e.g.* [23, 28] for details. The scaling exponent function $\tau(q)$ for $q \to \infty$ should be linear with the coefficient $-\ln(m)/\ln(2)$,

and for $q \to -\infty$ should be linear with the coefficient $-\ln(1-m)/\ln(2)$. In Fig. 2 we see that there are two peaks corresponding to the two limiting linearities of $\tau(q)$ in pdfs, only if the interval of $|q|$ is large enough. If q-interval is too narrow, *e.g.*, $|q| < 3$, then the distribution of $\{h_i\}$s becomes almost uniform.

In summary, there are at least two sources of the spectrum accumulation points. The crucial one is related to the intrinsic properties of a signal and it provides the characterization to a multifractal spectrum. The second source is the linearization effect which is related to limits of multifractal formalism. The linearization effect is absent in the case of multifractality of the binomial cascade type, but in the case of self-similar signals this effect is present, especially in the WTMM spectra received from integrated signals. But by observing emergence and/or disappearance of the spectrum accumulation points when q-interval is changed, the monofractality of fBm_H type can be clearly distinguished from the multifractality of the binomial cascade type.

2.4. Spectrum accumulation points in LF, VLF, ULF bands

Now we test the possibility of observing the monofractal indiced (a)–(c) in signals when mulifractal formalism is considered in the LF, VLF and ULV bands separately. The tests of MDFA and WTMM estimators were performed as follows. 50 samples (consisting of 25000 points) for each process fBm_H with $H = 0.1, 0.2, ..., 0.9$ were prepared by [31]. For each sample the partition functions $Z(n,q)$ and $F(n,q)$ for direct signals and $Z^{\mathrm{int}}(n,q)$ and $F^{\mathrm{int}}(n,q)$ for integrated signals, were found for $n \geq 10$ and $q \leq 5$ with a step $\Delta q = 0.1$ (software packets of Physionet [32] were used). Then the group averages $\langle Z(n,q)\rangle_H$, $\langle Z^{\mathrm{int}}(n,q)\rangle_H$, $\langle F(n,q)\rangle_H$ and $\langle F^{\mathrm{int}}(n,q)\rangle_H$ were calculated. For each group average, the scaling functions $\tau(q)$ were found separately in each scaling interval: LF, VLF and ULF. Finally, the multifractal formalism was applied to each $\tau(q)$.

In Fig. 3 we show the MDFA and WTMM spectra and the analysis of these spectra done by means of pdfs for $\mathrm{fBm}_{0.2}$ and $\mathrm{fBm}_{0.2}^{\mathrm{int}}$ signals. To observe emergence and disappearance of accumulation points, pdfs are calculated in two q-intervals: $q \leq 3$ and $q \leq 5$.

After change of the q-interval peaks corresponding the spectrum accumulation points emerge in all bands LF, VLF and ULF. A single h_{acc} can be attributed to each multifractal spectrum though in the case of some spectra the maxima are not sharp. Both estimators, when considered in the VLF band, give the spectrum accumulation points at values which are closely related to the expected values, *i.e.*, $h_{\mathrm{acc}} = 0.2$ for $\mathrm{fBm}_{0.2}$ signals and $h_{\mathrm{acc}} = 1.2$ for $\mathrm{fBm}_{0.2}^{\mathrm{int}}$ signals. But in the LF band, see circles (brown on-line) in Fig. 3, the MDFA spectrum does not give an evident single accumulation

spectrum point for $\mathrm{fBm}_{0.2}$ and provides h_{acc} at the wrong position in the case of $\mathrm{fBm}_{0.2}^{\mathrm{int}}$. The WTMM method works correctly in the LF band. The opposite observation holds in the ULF band, see squares (green on-line) in Fig. 3. Here the WTMM spectra provide wrong results but MDFA method finds h_{acc} close to the expected values.

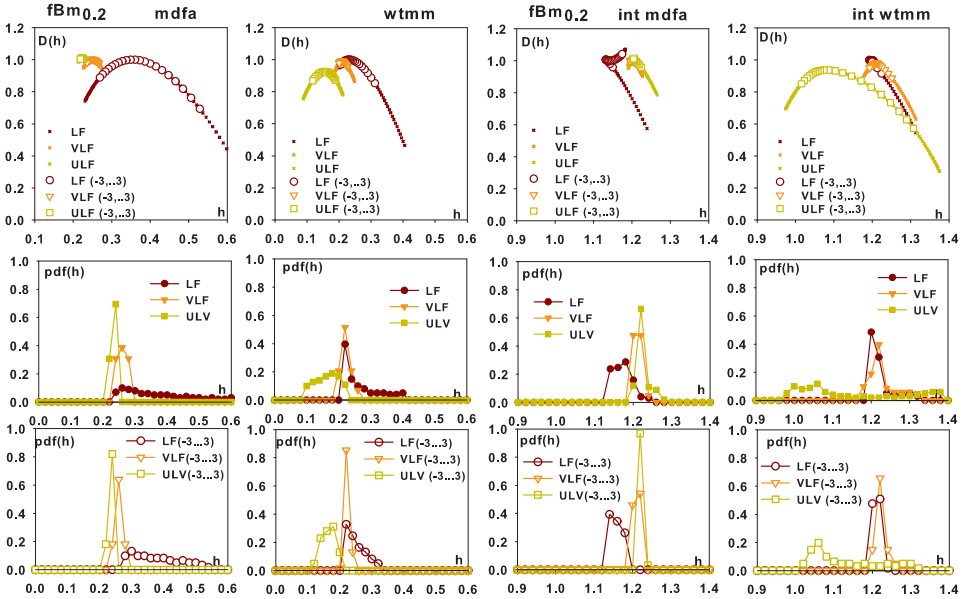

Fig. 3. Spectrum accumulation points in the case of $\mathrm{fBm}_{0.2}$. MDFA and WTMM spectra for pure and integrated signals are in the first row. Small markers correspond to spectra in $|q| < 5$, large markers to $|q| < 3$. The middle row presents pdfs for $|q| < 5$, the bottom row pdfs for $|q| < 3$.

In addition, thanks to a pdf we can easily estimate the spectrum width even a spectrum has a complicated shape. The influence of numerical instabilities leading to enormously large left or right wing can be limited by taking into account only values that are symmetrical with respect to the h_{acc}. Then the width of a spectrum in a given q-interval is calculated as the size of symmetric h interval where pdf is nonzero.

The results of analysis of properties (a)–(c) for all groups of fBm_H signals are collected in Fig. 4 and can be summarized as follows.

In the LF band the MDFA method finds multifractal spectra of fBm_H with $H < 0.6$ definitely different from the expected results. The spectra are enormously wide and the maxima are overestimated. When integrated signals are considered (the right column in Fig. 4) then the maxima are underestimated though the widths of the spectra are still large. Fortunately, in the VLF and ULF bands the MDFA spectra are located at the expected

values and they can be considered as a point-width spectra since their widths are less than about 0.05. In the case of the WTMM method, the spectra received in the ULF band are wrong. But WTMM spectra received in the LF and VLF intervals provide an acceptable picture of a point-like spectra.

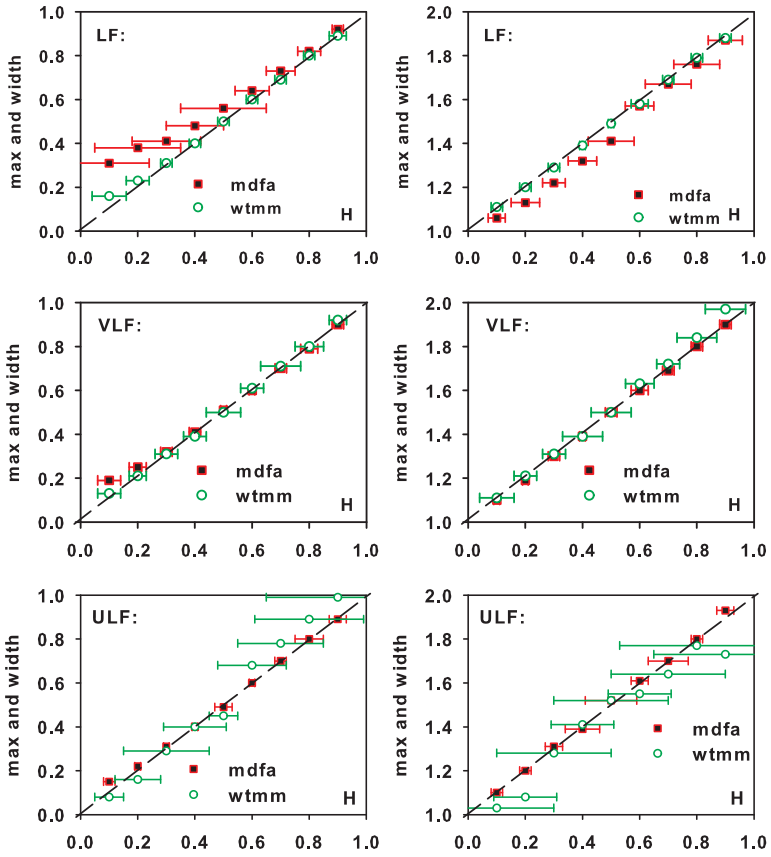

Fig. 4. Maxima (dots) and widths (arms) of mean spectra obtained by MDFA and WTMM estimators in power spectral bands LF, VLF and ULF for fBm_H series (left column) and integrated fBm_H (right column). $H = 0.1, 0.2 \ldots, 0.9$, $q \in [-5, 5]$. Dashed lines correspond to theoretical values.

For a comparison let us consider a binomial cascade signal, Fig. 5. In this case we see that each pdf has two accumulation points: left and right. Here the values of h_{acc} approximate correctly the known asymptotic values of multifractal spectra only if the MDFA method is used to VLF and ULV bands, and the WTMM method is used to LF and VLF.

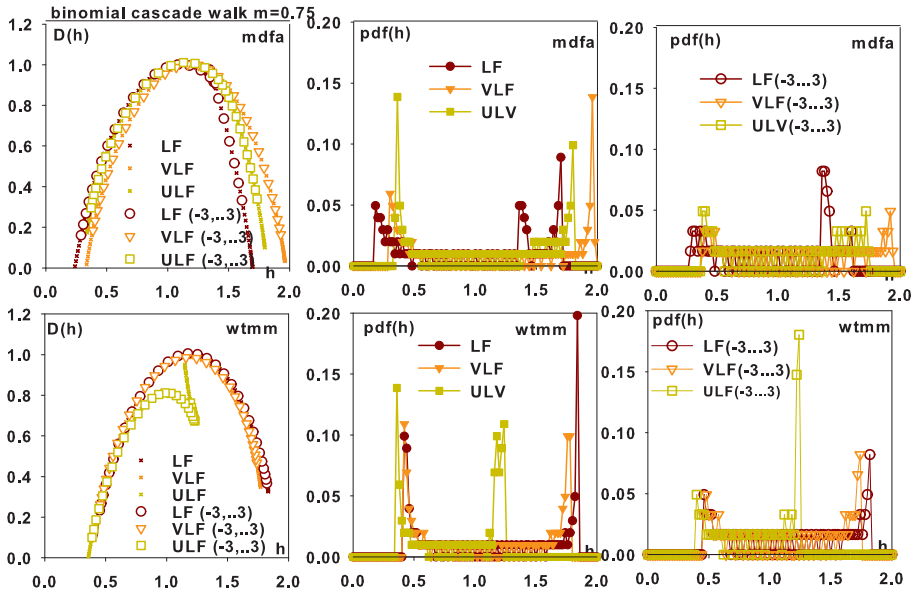

Fig. 5. Spectrum accumulation points in the case of a binomial cascade signal with $m = 0.75$. MDFA and WTMM spectra are in the first column. Small markers correspond to spectra in $|q| < 5$, large markers to $|q| < 3$. The middle column presents pdfs for $|q| < 5$, the left column pdfs for $|q| < 3$.

3. Heart rate variability by spectrum accumulation points in LF, VLF and ULV bands

At present we are well equipped to investigate sets of spectrum accumulation points describing multifractal features of a normal sinus rhythm (nsr). The signals were collected from 39 healthy individuals (characterization of this group can be found in [17]). From 24-hour electrocardiogram two subsets (of five hours long) were selected to separate the diurnal activity from nocturnal rest. These subsets will be referred to as *nsr_gda_wake* and *nsr_gda_sleep*, respectively. All series are accessible from [33].

For each signal $\mathrm{RR}(i)$ the corresponding integrated signal $\mathrm{RR}^{\mathrm{int}}(k) = \sum_{i=1,\ldots,k} \mathrm{RR}(i)$ was considered. Notice, that by integrating RR intervals we obtain a sequence of moments of time when a k-th heart beat happens.

Finally, from each 24-hour recording, the eight partition functions were calculated: $Z_{\mathrm{wake}}(n,q)$, $F_{\mathrm{wake}}(n,q)$, $Z_{\mathrm{sleep}}(n,q)$, $F_{\mathrm{sleep}}(n,q)$, $Z^{\mathrm{int}}_{\mathrm{wake}}(n,q)$, $F^{\mathrm{int}}_{\mathrm{wake}}(n,q)$, $Z^{\mathrm{int}}_{\mathrm{sleep}}(n,q)$, $F^{\mathrm{int}}_{\mathrm{sleep}}(n,q)$. The partition functions were found for $q \in [-5,5]$ with a step $\Delta q = 0.1$ and $n \geq 10$. The individual functions were averaged in the eight groups to establish one representative for each group (one can learn more about the group representatives and other details of

numerical and statistical procedures from [30]). The multifractal formalism was applied to each group representative and in each of LF, VLF and ULF band. In Figs. 6–8 the MDFA and WTMM spectra are presented.

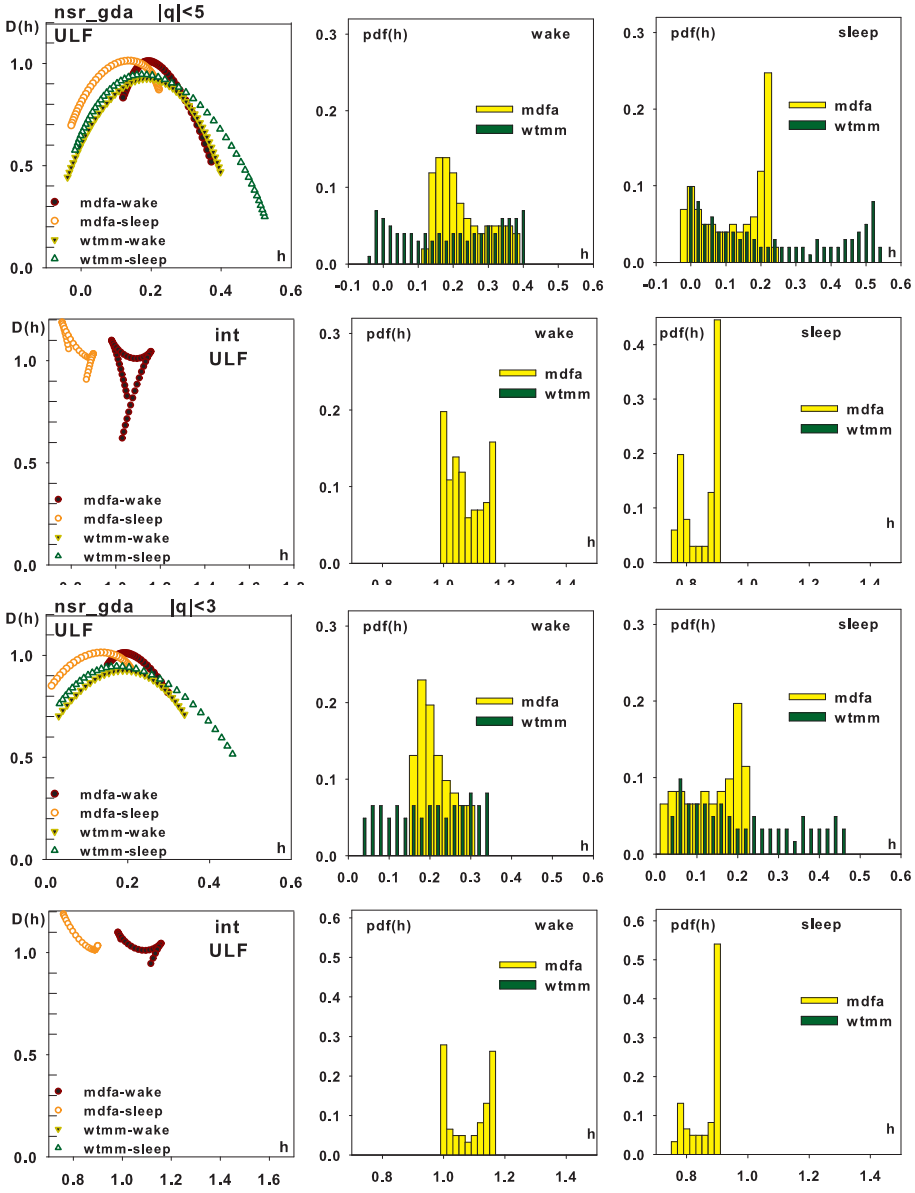

Fig. 6. MDFA and WTMM spectra (the first column) and pdfs found accordingly for *wake* and *sleep*, and direct and integrated series in the ULF band. Two q intervals are considered $|q| < 5$- upper panels and $|q| < 3$ bottom panels.

The ULF component corresponds to the long-time control of ANS and in this time interval the multifractal properties are usually investigated. In the case of a healthy heart, the standard multifractal estimates of RR-intervals give a nocturnal multifractal spectrum wider than diurnal one, and with maximum moved to lower values of h. This picture of the circadian rhythm is said to reflect the known physiological fact about stronger HRV during the sleep.

In Fig. 6 one can find these properties in MDFA and WTMM spectra received by us in the ULF band. Remembering that the WTMM method is partially reliable in the ULF band, it is worth to notice that values of the maxima in MDFA and WTMM spectra are close to each other. They appear at about 0.20. The spectrum accumulation points calculated from the *wake* MDFA spectrum indicate at a single h_{acc} at about 0.20. For integrated *wake* series, the MDFA method provides two accumulation points which values are close each other, and one of them is $h_{\mathrm{acc}} \approx 1.2$. Hence, basing on our experience with fBm_H, we can hypothesis that in this band the dynamics of ANS control can be described by a process of a monofractal type. The self-similarity index for this process is about $H = 0.20$.

The nocturnal HRV in the ULV band does not allow for such simple description. A strong spectrum accumulation point at 0.2 is still observed in the pdfs. But the integrated *sleep* signals provide the MDFA spectra with all $h < 1$ what disagrees with property (c) of fBm_H.

A first message which can be read from Fig. 7 is that in the VLF band the multifractal spectra of RR-signals depend on the applied method. The WTMM spectra are separated systematically from MDFA spectra — they are moved to left, *i.e.*, to lower values of h. It looks like the WTMM method finds RR-signals to be more rough. However, if estimates are performed on integrated signals then both methods find a consistent with each other multifractal picture. For example, we see a clear separation between the maxima of multifractal spectra representing *wake* and *sleep* signals.

One can search for an explanation to the described result in numerical procedures which are involved, compare Section 2.1. In general, the WTMM method is concentrated on taking out singularities across scales while the MDFA method measures departures from a local polynomial trend in a given scale. In the case of fBm_H where trends are absent, both methods give the same multifractal characterization. In addition, if a strong trend is imposed on a signal, *e.g.*, by integrating values of a signal, then this discrepancy vanishes. Therefore one can suppose that the difference between MDFA and WTMM spectra is observed if a signal has complicated other than polynomial dependences.

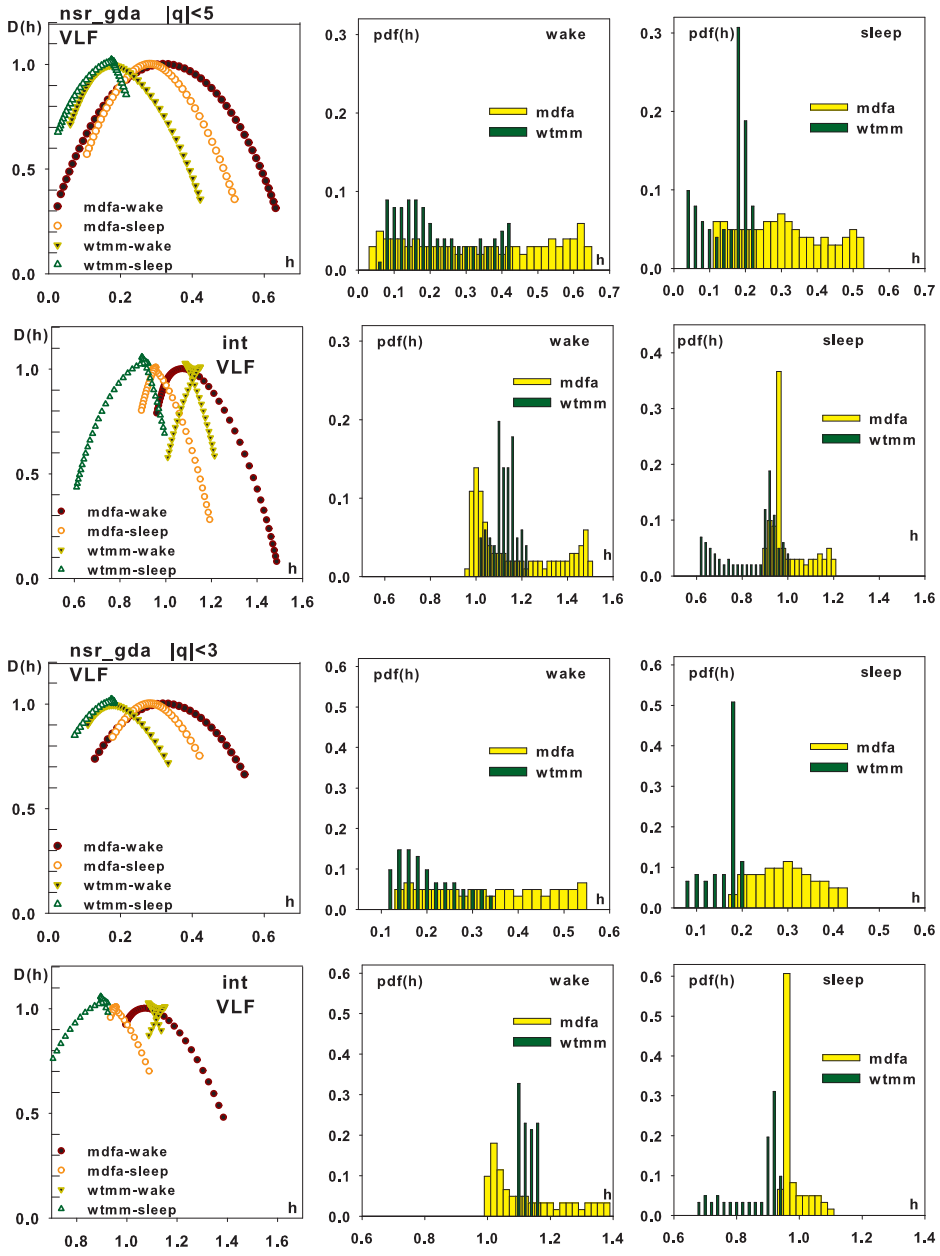

Fig. 7. MDFA and WTMM spectra in the VLF band. The plots are arranged in the same way as in Fig. 6.

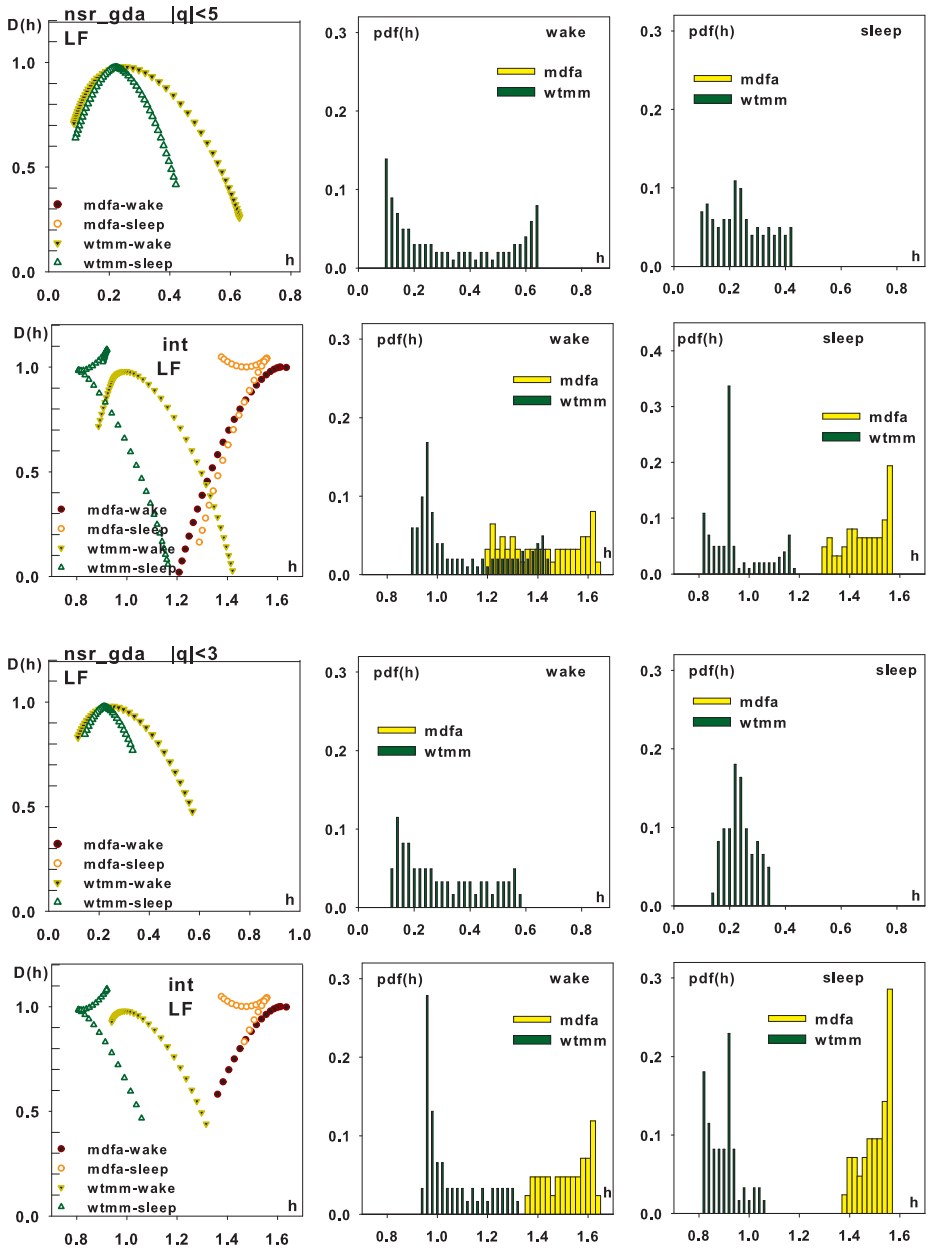

Fig. 8. MDFA and WTMM spectra in the LF band. The plots are arranged in the same way as in Fig. 6.

The MDFA spectra in the VLF band provide wide and almost uniformly distributed pdfs for *wake* and *sleep* signals independently of q-interval. Such shape indicates that an RR signal could be compared to a binomial cascade signal. The pdfs received for integrated signals are also wide though, here, a strong single spectrum accumulation point $h_{\mathrm{acc}} \approx 1.0$ is present. Also, the pdfs obtained from WTMM spectra (from direct and integrated signals) suggest a monofractal representation to physiological processes involved in *wake* activity in this band. This driving process can be assessed as $H \in (0.1, 0.2)$. But, similarly to the observations found in the ULF band, in the case of *sleep* signals we cannot describe the main process as a monofractal type because the direct signals give $H = 0.18$ while integrated signals lead to $H = 0.92$, *i.e.*, to the value smaller than 1.

In the LF band, see Fig. 8, the MDFA method is partially reliable only. Discussing results offered by WTMM method we see that the maxima in nocturnal WTMM spectra are attained at the similar values as in diurnal WTMM spectra when direct signals are considered. Moreover, the *sleep* spectra are narrower than the *wake* spectra what is opposite to findings reported in the ULF band. The *wake* signals provide a wide spectrum limited by easily seen two accumulation spectrum points. These points survive the change in q-interval what indicates that they are not related to the linearization effect but they represent the intrinsic organization of the data in *wake* signals. In the case of *sleep* series we observe only one h_{acc} point if $|q| \leq 3$ what suggests existence of strong driving monofractal ingredient. However, pdf obtained for integrated *sleep* signals is moved right only by about 0.80 what locates the spectrum below 1. As it was mentioned earlier, such values disagree with the property (c) of monofractals. Hence here in the LF band both ANS states: diurnal and nocturnal, cannot be described as a monofractal process of fBm_H type.

4. Conclusions

The hypothesis was tested, whether the multifractal analysis can be performed in fixed intervals of scaling procedure, in the aim to find a new source of indices for ANS control of heart rate. For this reason the intervals for scaling were selected to LF, VLF and ULV bands, to be suitable for diagnostic interest of cardiologists. Moreover, the search for the dominating process responsible for HRV within the several seconds (LF), less than a minute (VLF), and few minutes (ULF), is crucial in simplifying our understanding of the complexity in HRV.

Since the best numerical tools for multifractal analysis: WTMM and MDFA are heuristic, the validation of the hypothesis was given by tests on signals with known multifractal properties. We practiced with signals of fractional Brownian motions and binomial cascade. The robust method:

markers (a)–(d), was proposed to detect and quantify monofractal properties by multifractal tools. The performed analysis provided us the following arguments about the quality of WTMM and MDFA methods as estimators of monofractality in a signal:

(i) Both methods when applied to the VLF band, provide values correctly related to the expected ones.

(ii) In the ULF band, the WTMM method wrongly finds signal properties while MDFA is a good estimator.

(iii) In the LF band, the MDFA method does not estimate correctly multifractal spectra but the WTMM method works well.

Let us draw attention to the result *(ii)*. Our observation could be a possible explanation to a rather common judgment that the WTMM method is a worse estimator of multifractality than the MDFA method [17, 28, 29].

Because an answer to the hypothesis has to be read as 'yes, though with care', we have gained a delicate tool to study RR-intervals in time scales of physiological interest. A promising way to find new methods to evaluate the state of the ANS control has been established.

We have found that the ANS control during the human daily activity in the ULF band can be described by a process of a monofractal type. It means that in scales of minutes the HRV complexity can be approximated by some self-similar process with self-similarity index $H \approx 0.2$. But in short time scales which correspond to the LF band we obtain a multifractal picture of ANS activity. Hence a transition is found in the dynamic organization of ANS control connected to the change in time scales. In the effect of this transition the switch in the relation between widths of *wake* and *sleep* multifractal spectra is observed. In the LF band the wider multifractal spectra are attributed to diurnal activity, while in the ULF band the nocturnal RR-signals lead to wider spectra.

One can object that our observations are restricted to the numerical tools that we have used, namely, tsfBm packet [31] as generator of fBm_H signals and multifractal software from the Physionet [32]. However, the similar properties have been received when series were obtained by different fBm_H generators and different numerical representations of WTMM and MDFA estimators are used [34].

We kindly acknowledge Dr. P. Oświęcimka for performing tests, with other series and other numerical tools, supporting our observations. The work is supported by the Polish Ministry of Higher Education and Science — PB: 1921/B/H03/2008/34.

REFERENCES

[1] *Heart Rate Variability. Standards of Measurement, Physiological Interpretation, and Clinical Use*, *Eur. Heart J.* **17**, 354 (1996).

[2] M.J. De Jong, D.C. Randall, *J. Cardiovasc. Nurs.* **20(3)**, 186 (2005).

[3] M.P. Freneaux, *Heart* **90(11)**, 1248 (2004).

[4] M.E. Gregory, R.J. Cody, E. Nuziata, P.F. Binkley, *Circulation* **92**, 551 (1995).

[5] G.R.H. Sandercock, D.A. Brodie, *Pacing Clin. Electrophysiology* **29(8)**, 892 (2006).

[6] M. Kobayashi, T. Musha, *IEEE Trans. Biomed. Eng.* **BME-29**, 456 (1982).

[7] C.K. Peng, J. Mietus, J. Hausdorff, S. Havlin, H.E. Stanley, A.L. Goldberger, *Phys. Rev. Lett.* **70**, 1343 (1993).

[8] Y. Yamamoto, R.L. Hughson, *Am. J. Physiol.* **266**, R40 (1994).

[9] T.H. Mäkikalio, J.S. Perkiömäki, H.V. Huikuri, in *Dynamic Elecrocardiogcraphy*, eds. M. Malik, A.J. Camm, Blackwell Futura, 2004, p. 22.

[10] P.Ch. Ivanov, M.G. Rosenblum, C.-K. Peng, J. Mietus, S. Havlin, H. E. Stanley, A.L. Goldberger, *Nature* **383**, 323 (1999).

[11] P.Ch. Ivanov, L.A. N. Amaral, A.L. Goldberger, S. Havlin, M.G. Rosenblum, Z.R. Struzik, H.E. Stanley, *Nature* **399**, 461 (1999).

[12] M. Meyer, O. Stiedl, *Eur. J. App. Physiol.* **90**, 305 (2003).

[13] Z.R. Struzik, J. Hayano, S. Sakata, S. Kwak, Y. Yamamoto, *Phys. Rev.* **E70**, 050901-1(R) (2004).

[14] K. Kotani, Z.R. Struzik, K. Takamasu, H.E. Stanley, Y. Yamamoto, *Phys. Rev.* **E72**, 041904-1 (2005).

[15] D. Makowiec, R. Gałązka, A. Dudkowska, A. Rynkiewicz, M. Zwierz, *Physica A* **369**, 632 (2006).

[16] S. Cerutti, F. Esposti, M. Ferrario, R. Sassi, M.G. Signorini, *Chaos* **17**, 015108-1 (2007).

[17] R. Gałązka, D. Makowiec, A. Dudkowska, A. Koprowski, K. Chlebus, J. Wdowczyk-Szulc, A. Rynkiewicz, *Annals of Noninvasive Electrocardiology* **13**, 155 (2008).

[18] D. Roach, A. Sheldon, W. Wilson, R. Sheldon, *Am. J. Physiol.* **274**, H1465 (1998).

[19] C.-K. Peng, S. Havlin, H.E. Stanley, A.L. Goldberger, *Chaos* **5(1)**, 82 (1995).

[20] J.S. Perkiömäki, V. Jokinen, J. Tapanainen, K.E. Airaksinen, H.V. Huikuri, *Ann. Noninvasive Electrocardiol.* **13(2)**, 120 (2008).

[21] F. Beckers, B. Verheyden, A.E. Aubert, *Am. J. Physiol. Heart Circ. Physiol.* **290**, H2560 (2006).

[22] L. Glass, *Chaos* **18**, 020201 (2008).

[23] R.H. Riedi, *Multifractal Processes*, in *Long-Range Dependence: Theory and Applications*, eds. P. Doukhan, G. Oppenheim, M.S. Taqqu, Cambridge Ma, Birkhäuser, 2001, p. 625.

[24] W. Willinger, V. Paxson, R.H. Riedi, M.S. Taqqu, in *Long-Range Dependence: Theory and Applications*, eds. P. Doukhan, G. Oppenheim M.S. Taqqu, Cambridge Ma, Birkhäuser, 2001, p. 1.

[25] A. Eke, P. Herman, L. Kocsis, L.R. Kozak, *Phys. Meas.* **23**, R1 (2002).

[26] P. Abry, S. Jaffard, B. Lashermes, *Optic East, Wavelet Applications in Industrial Applications II*, vol. 5607, Philadelphia, USA, 2004.

[27] E. Bacry, J.F. Muzy, A. Arnedo, *J. Stat. Phys.* **70**, 635 (1993); J.F. Muzy, E. Bacry, A. Arneodo, *Phys. Rev.* **E47**, 875 (1993).

[28] J.W. Kantelhardt, S.A. Zschiegner, E. Koscielny-Bunde, S. Havlin, A. Bunde, H.E. Stanley, *Physica A* **316**, 87 (2002).

[29] P. Oświęcimka, J. Kwapień, S. Drożdż, *Phys. Rev.* **E74**, 016103-1 (2006).

[30] D. Makowiec, A. Dudkowska, R. Gałąska, A. Rynkiewicz, `arXiv:q-bio/070204`.

[31] J. Conove, `http://www.johncon.com/`

[32] A.L. Goldberger, L.A.N. Amaral, L. Glass, J.M. Hausdorff, P.Ch. Ivanov, R.G. Mark, J.E. Mietus, G.B. Moody, C.-K. Peng, H.E. Stanley, *Circulation* **101(23)**, e215 (2000), `http://circ.ahajournals.org/cgi/content/full/101/23/e215`.

[33] RR series and MDFA software can be downloaded from `http://iftia9.univ.gda.pl/~danka/DATA`

[34] P. Oświęcimka, private communication.